Topological reorganization of functional hubs in Parkinson's disease patients with freezing of gait.

Virendra Mishra (mishrav@ccf.org)
Lou Ruvo Brain Institute https://orcid.org/0000-0002-0452-6400

Karthik Sreenivasan
Cleveland Clinic Lou Ruvo Center for Brain Health https://orcid.org/0000-0002-6486-302X

Ece Bayram
University of California San Diego

Xiaowei Zhuang
Cleveland Clinic Lou Ruvo Center for Brain Health

Jason Longhurst
Saint Louis University

Zhengshi Yang
Cleveland Clinic Lou Ruvo Center for Brain Health

Dietmar Cordes
Cleveland Clinic Lou Ruvo Center for Brain Health

Aaron Ritter
Cleveland Clinic Lou Ruvo Center for Brain Health

Jessica Caldwell
Cleveland Clinic Lou Ruvo Center for Brain Health

Jeffrey Cummings
University of Nevada, Las Vegas

Zoltan Mari
Cleveland Clinic Lou Ruvo Center for Brain Health https://orcid.org/0000-0003-0356-9879

Irene Litvan
University of California San Diego

Brent Bluett
Central California Movement Disorders

Article

Keywords: Functional connectivity, Freezing of gait, Parkinson's disease, Graph theory, functional Magnetic Resonance Imaging.

Posted Date: May 31st, 2022

DOI: https://doi.org/10.21203/rs.3.rs-1409611/v1

Abstract

Resting-state functional MRI (rs-fMRI) studies in Parkinson's disease (PD) patients with freezing of gait (FOG) have implicated dysfunctional connectivity over multiple resting-state networks. While these findings provided information related to the aberrant or altered regional functional connectivity, whether these alterations have any effect on topological reorganization in PD-FOG patients is incompletely understood. In this study, we use rs-fMRI data and graph theoretical approaches to explore the reorganization of resting-state network topology in PD-FOG when compared to those without FOG (PD-nFOG). We found that the PD-FOG patients showed global topological reorganization accompanied by a reduction in efficiency and network strength. There was also a noticeable reorganization of 'hub' regions and significantly reduced rich-club connectivity in PD-FOG. Overall our findings demonstrate a widespread topological reorganization in PD-FOG which may further assist in improving our understanding of functional network disturbances associated with PD-FOG.

1. Introduction

Freezing-of-gait (FOG) is defined as a brief, episodic absence or marked reduction of the forward progression of feet despite the intention to walk (Allen et al., 2013). Parkinson's disease (PD) patients with this syndrome experience a feeling that their feet are "glued" to the floor and are unable to move (Allen et al., 2013). In PD patients FOG is one of the most common causes of falls and subsequent morbidity and mortality (Snijders et al., 2011). FOG has been attributed to overloading across neural networks in an attempt to compensate for reduced motor function (Bluett et al., 2018; Browner and Giladi, 2010; Naismith et al., 2010; Shine et al., 2013a) which may lead to the inability to "set-shift" between motor and cognitive tasks observed in PD-FOG (Naismith et al., 2010).

Neuroimaging studies, including resting-state functional MRI (rs-fMRI), have implicated altered connectivity in the motor and non-motor pathways and dysfunctional connectivity between cortical and subcortical regions over multiple resting-state networks (RSNs) (Bharti et al., 2019; Fasano et al., 2015). Specifically, resting-state functional connectivity (rs-FC) involving the frontoparietal network and visual network was altered in PD-FOG and this disruption of connectivity between RSNs was correlated with FOG (Bharti et al., 2019). Recent studies have augmented these findings and have shown the involvement of the sensorimotor, dorsal attention, and default mode networks (Maidan et al., 2019; Ruan et al., 2020). Although most studies show a correlation between the severity of FOG symptoms and aberrant or altered regional functional connectivity, whether these observed changes in resting-state functional connectivity alters the network organization in PD-FOG remains poorly understood.

Advances in the application of graph-theoretical methods have enabled us to characterize unbiased whole-brain connectivity at global and local levels and gain insights into the topological organization of the human brain networks (Achard et al., 2006; Bassett et al., 2008; Bullmore and Sporns, 2009; Sporns et al., 2005). Previous studies have demonstrated large-scale network changes from early brain development to healthy aging and various neurodegenerative diseases. For instance, the graph-

theoretical methods have contributed to our understanding of brain organization from infants (Cao et al., 2017) to healthy aging (Perry et al., 2015), as well as in various neurological disorders (Bachmann et al., 2018; Caeyenberghs et al., 2017; Caliandro et al., 2017; Gleichgerrcht et al., 2015; Mishra et al., 2020; Rocca et al., 2016; Sreenivasan et al., 2019). Graph-theoretical approaches can be used to study various network measures that can inform about both network segregation and integration (Rubinov and Sporns, 2010). Limited existing studies have adopted a whole-brain unbiased approach to study network-level connectivity differences related to PD-FOG, and these have shown altered topological organization at the network and regional level (Guo et al., 2020; Li et al., 2021; Ruan et al., 2020). One study looking at network-specific organizations showed reduced efficiency of the dorsal attention network (Maidan et al., 2019) in FOG participants compared to PD participants without FOG (PD-nFOG) and normal controls (NCs). However, such network-specific insights do not explain the higher-order functional organization, which could be derived from the 'hub' and the 'rich-club' organization of functional networks. Nodes in a network that are identified as hubs or part of a rich club are proposed to be vital for global network integration and coordination(van den Heuvel and Sporns, 2013, 2011). The hub nodes play an important role in global integration and the rich-club organization can provide insights into the network's resilience, hierarchical ordering, and specialization (van den Heuvel and Sporns, 2013, 2011). Subsequently, given that PD-FOG is associated with the inability to "set-shift" among different executive tasks, understanding the role of key hub-like regions that play an important role in the efficient global integration of brain functional networks could be crucial to identifying the distinct and unique pattern of the network connectivity associated with PD-FOG.

In this study, we used high temporal resolution rs-fMRI data to investigate whether there are discernible topological organization differences between PD patients with and without FOG. We applied the graph-theoretical approach to the functional connectivity data derived using rs-fMRI and first compared global and local graph-theoretically derived topological measures of efficiency between the groups, and evaluated whether these measures were different between the two groups. We also computed and compared hub and rich-club measures in the functional connectivity networks of these PD-FOG participants to understand whether there is a topological reorganization of these hubs in PD-FOG participants.

2. Materials And Methods

Data used for this study were obtained from the Center for Neurodegeneration and Translational Neuroscience (CNTN) database (www.nevadacntn.org). The current study was approved by the institutional review board of Cleveland Clinic and all subjects provided informed written consent. Inclusion criteria for PD patients in this study was a diagnosis of PD based on the United Kingdom Parkinson's Disease Society Brain Bank Diagnostic Criteria. PD participants were evaluated for FOG with a self-report measure (FOGQ) and a comprehensive battery of clinical tests (FOG score (Ziegler et al., 2010) including Timed Up and Go and Movement Disorders Society-Unified Parkinson's Disease Rating Scale (MDS-UPDRS III)). These assessments were recorded and reviewed by three members of the research team (two movement disorders specialists and one physical therapist with expertise in FOG) to

confirm the presence or absence of FOG. Participants were classified to have FOG if they were observed to have a FOG episode during any of the clinical assessments for FOG. Thirty-eight PD participants were recruited; 17 participants were identified as PD-FOG and as 21 PD-nFOG. Of these 1 PD-FOG and 5 PD-nFOG participants were identified as outliers based on Movement Disorders Society-Unified Parkinson's Disease Rating Scale (MDS-UPDRS III) scores and were removed from further analysis. We included 16 NCs as a comparison group. We obtained general demographics for all subjects and the disease duration, Montreal Cognitive Assessment (MoCA), Freezing of Gait Questionnaire (FOGQ) score, Hoehn and Yahr scale, and MDS-UPDRS-III scores (ON and OFF state) for each PD patient (Table 1).

Table 1

Demographics. Various demographics along with UPDRS in ON state (PD subjects only) are shown along with their mean ± SD. Statistical comparison was conducted for every demographic and the values are shown as p-values.

Demographics	**Controls (n = 16)**	**PD-nFOG (n = 16)**	**PD-FOG (n = 16)**	**p-value**
Age (Years)	68.50 ± 4.29	67.56 ± 6.63	69.43 ± 7.22	0.73
Sex (M: Males; F: Females)	9M; 7F	10M; 6F	13M; 3F	0.29
Handedness **R = Right-handed; L = Left-handed**	16R	14R; 2L	15R; 1L	0.34
Years of Education	16.19 ± 1.47	16.19 ± 2.19	14.93 ± 2.41	0.14
Montreal Cognitive Assessment (MoCA)	26.50 ± 2.66	26.37 ± 2.47	24.75 ± 2.41	0.07
Hoehn and Yahr scale (1/2/3)	-	0/16/0	0/13/3	0.07
Disease Duration	-	7.25 ± 3.29	9.48 ± 4.56	0.10
Freezing of Gait Questionnaire (FOGQ)	-	*3.99 ± 5.06*	*30.83 ± 10.54*	< 0.001
MDS-sponsored Unified Parkinson's Disease Rating Scale-III (ON-state)	-	*18.12 ± 3.65*	*25.53 ± 7.72*	0.001

All subjects underwent rs-fMRI scans on a 3T Siemens scanner. A 32-channel head coil was used for data acquisition, and all PD participants were scanned in the clinically defined 'ON' state. The rs-fMRI involved gradient-echo T2*-weighted echo-planar imaging (EPI) acquisition with 850-time points (TR = 700ms, TE = 28.4ms, flip angle = 42°, resolution = 2.3x2.3x2.3mm^3, 64 axial slices, multiband = 8, and phase encoding = P > > A). We acquired spin-echo EPI images with the same parameters in the same and opposite phase encoding (P > > A and A > > P respectively) for distortion correction. A high resolution

(1x1x1mm^3) T1-weighted structural image was acquired for each subject using a T1- weighted gradient echo 3D with magnetization-prepared 180 degrees radio-frequency pulses and rapid gradient-echo (MP-RAGE) sequence (TR = 2300ms, TE = 2.96ms, flip angle = 9°). The total time of acquisition was approximately 18 minutes.

The first 15 time frames (10 sec) were removed to allow the MR signal to achieve T1 equilibrium. Time frames were distortion corrected, slice-time corrected, and realigned to the mean image using the statistical parametric mapping (SPM12) (http://www.fil.ion.ucl.ac.uk/spm/), further co-registered to the subject T1-space, and then normalized to the standard MNI-152 2mm-template using advanced normalization tools (ANTs) (http://stnava.github.io/ANTs/). 242 different cortical regions of interest (ROIs) were identified based on the Brainnetome functional atlas (Fan et al., 2016). The first principal component resulting from the singular value decomposition of all the time-series within the region of interest (ROI) mask was defined as the time-series for the ROI. Six motion parameters and their derivatives, as well as CompCor generated white-matter (WM) and cerebrospinal (CSF) signals (Behzadi et al., 2007), were regressed from the extracted time-series. All voxel time-series were bandpass filtered (0.008Hz < f < 0.1Hz) to emphasize low-frequency correlations in the resting state, and then variance normalized. Root-mean-square (RMS) head motion was computed for every subject.

The extracted and pre-processed time series were then used to obtain functional connectivity (FC) matrices for all participants. Pearson correlation coefficient between the time-series for each pair of ROIs was calculated and the correlation matrix was obtained for each subject.

Graph-theoretical measures were used to study the topological properties of functional networks in the different groups. The correlation matrices obtained were thresholded by sorting all the edges by weight (highest correlation to lowest correlation) and only retaining the top S% of edges (S = sparsity). Subsequently, we ensured that the thresholded set of weighted graphs being compared had the same number of edges to determine unbiased between-group differences in network organization (Achard and Bullmore, 2007). Only positive correlation values (r-values) were used for the analysis. The thresholding was applied for a range of S values with an interval of 0.01. The lower limit of 0.1 (10%) was chosen such that nodes that are isolated from the rest of the network are minimal, and the upper limit of 0.5 (50%) was chosen to suppress the contribution of spurious correlations, similar to previous studies (He et al., 2008; Sreenivasan et al., 2019). Graph-theoretical measures used to compare group differences were obtained using custom Matlab® scripts and graph-theoretical network analysis (GRETNA) toolbox(Wang et al., 2015).

The network measures of interest namely: (1) Small-world properties (including normalized weighted clustering coefficient (γ), and normalized weighted characteristic path length (λ)), (2) network efficiency involving local efficiency (E_{loacl}) and global efficiency (E_{global}), (3) network strength (D), and (4) assortativity (A) (Bullmore and Sporns, 2009) were calculated at each S. In addition, we also estimated the hub-disruption index (Achard et al., 2012) and the rich-club properties (van den Heuvel and Sporns, 2011).

Small-world properties

Small-world properties were originally proposed by Watts and Strogatz (Watts and Strogatz, 1998). It involves the determination of the clustering coefficient (C), characteristic path length (L), γ, and λ. C denotes the extent of local interconnectivity or cliquishness in the network and was measured by taking the average of clustering coefficients across all nodes in the network. γ was computed by normalizing each graph's C by C_{random} (mean C of 100 matched random networks). L of the network was computed as the average of the shortest path length, averaged over all pairs of nodes in the network. λ was computed by normalizing each graph's L by L_{random} (mean L_{nw} of 100 matched random networks). The small-worldness of a network can be expressed as $\sigma = \gamma/\lambda$, which is typically larger than 1 in the case of a small-world organization ($\sigma > 1$; $\gamma > 1$ and $\lambda \sim 1$) (Achard et al., 2006; Watts and Strogatz, 1998). It represents both efficient network segregation and network integration (Rubinov and Sporns, 2010).

Network efficiency

Network efficiency was studied by obtaining local (E_{local}) and global efficiency (E_{global}) of the connectivity networks. The global efficiency E_{global} of the network measures the efficiency of the parallel information transfer and is given by the average of the inverse shortest path between the nodes in the network. E_{local} represents how well local subgraphs (sub-network) exchange information when the node under consideration is eliminated. E_{local} of the network provides information about network resilience to fault tolerance and is given by the average E_{global} within a local subgraph consisting only of the neighbors of a given node.

Network Strength

Network strength (D) measures indicate the strength of connectivity (amount of information transfer) in the corresponding network. D was calculated as the averaged degree over all the nodes in the network.

Assortativity

Assortativity (A) is a measure that assesses the tendency of a node being connected or disconnected to nodes of a similar degree (similar number of edges) in a network. A positive value of A indicates that nodes are likely to be connected to other nodes with the same degree and therefore hubs of the network are likely to be connected. If A is negative this implies that the hubs of the network are not connected. A was calculated as the correlation between the degree of a node and the mean degree of its nearest neighbors (Newman, 2002).

Hub-disruption index: Human functional brain networks comprise several highly connected hub nodes (van den Heuvel and Sporns, 2013), and to investigate the potential reorganization of these hubs in the PD-FOG participants we calculated the hub disruption index across three different groups. The hub disruption index (κ) provides a measure of change in the overall organization of brain hubs (Achard et al., 2012) and was calculated as the slope of the line fitted to the scatterplot of the average nodal strength

between the reference group and the difference between the reference group and chosen group. In the current study κ was calculated for three different comparisons: (a) The NCs as the reference group and PD-FOG as the chosen group (b) NCs as the reference group and PD-nFOG as the chosen group and (c) PD-nFOG as the reference group and PD-FOG as the chosen group. We used permutation testing to confirm the statistical significance (p_{corr}<0.001) of the observed slope i.e. κ. Subjects were arbitrarily assigned to different groups and one group was defined as the reference group and the other as the chosen group and the κ was calculated using the process described above. The permutation was repeated 10,000 times to generate the null distribution of κ (Suppl. Figure 1).

Rich-club properties

Rich-club is formed when the high-degree (nodes that have a large number of edges) nodes of a network tend to be more densely interconnected rather than with nodes that have a lower degree. The rich-club coefficient (ϕ), was calculated as the fraction of the number of existing edges for nodes with a degree larger than k, divided by the number of possible connections among these nodes. The ϕ was normalized using 100 matched random networks (ϕ_{rand}) and the ϕ_{norm} (ϕ/ϕ_{rand}) was obtained for each participant. A value of $\phi_{norm} > 1$ over a range of k was said to reflect the existence of a rich-club organization in a network. To understand whether there is a difference in the rich-club functional organization average rich-club edge strength, feeder edge strength, and local edge strength was then computed (van den Heuvel and Sporns, 2011). For each group, the presence of rich-club was assessed using the group average connectivity matrix. At the range of k where $\phi_{norm} > 1$ (i.e. expressing rich-club organization), it was tested whether ϕ was significantly greater than the ϕ_{rand}. The maximum degree (k_{max}) at which $\phi > \phi_{rand}$ in all the three groups was defined as the threshold where the “rich-club” properties were obtained. At the individual subject level, all rich-club measures were extracted and compared for differences in the rich-club properties for nodes with degrees greater than k_{max}.

Network-level differences in overall topological characteristics were studied by comparing the integrated area under the curve (AUC) metrics over the whole range of S (0.1:0.01:0.5) (Achard and Bullmore, 2007). Rich-club properties and related measures were compared at the minimum sparsity level at which the network was fully connected for all groups (He et al., 2008).

The Chi-square test and the Mann-Whitney U test were used to test the significance of demographic variables, clinical variables, and head motion. All comparisons were done between the three different groups ((NC vs PD-NFOG; NC vs PD-FOG and PD-NFOG vs PD-FOG). Nonparametric statistical analyses of group differences in graph-based metrics and correlation with clinical variables were conducted using the permutation analysis of linear models (PALM) toolbox in FSL (Winkler et al., 2014). Significance for PALM was established at family-wise error correction (FWE) p_{corr}<0.05.

3. Results

3.1. Demographics and Clinical measures

None of the demographic variables were significantly different between the groups (Table 1). All subjects had less than one voxel size RMS head motion and this measure was not significantly different between the groups. As expected, the PD-FOG participants had significantly higher FOGQ and MDS-UPDRS-III “ON” scores compared to the PD-nFOG participants. There were no between-group differences in MoCA, disease duration, or Hoehn and Yahr stage (Table 1).

3.2. Altered global information processing in PD-FOG

All three groups exhibited small-world properties. However, the PD-FOG participants showed an increase in the γ and a significantly reduced λ which was reflected in a significantly higher σ when compared to the NC (Fig. 1a-c). PD-FOG also showed increased γ and σ compared to the PD-nFOG participants. The E_{global}, E_{local}, S, and A were significantly reduced in PD-FOG participants compared to the NCs (Fig. 1) but did not survive adjustment for multiple comparisons. However, there was a trend (Fig. 1) of decreased E_{global}, E_{local}, S, and A in PD-FOG compared to the PD-nFOG participants.

3.3. Reorganization of functional hubs in PD-FOG

When compared to the NCs, both PD-FOG and PD-nFOG participants exhibited a significant reorganization of functional hubs as evaluated through the hub disruption index (Fig. 2). The group average hub disruption index showed a significant negative slope for the NC v/s PD-FOG and PD-nFOG v/s PD-FOG comparisons (Fig. 2a, c). Specifically, when comparing the PD-FOG participants against the NC, hub alterations were most evident for several regions of the visual, auditory and sensory/motor cortex, which all decreased their hubness. On the other hand, regions in the frontal cortex and inferior parietal lobe increased their hubness (Fig. 2a). Comparison of PD-FOG and PD-nFOG revealed a similar hub reorganization. Many regions of the sensory/motor cortex and parietal cortex showed a decrease in their hubness, and regions in the frontal cortex and inferior parietal lobe displayed increased hubness (Fig. 2c). Of note, the comparison between PD-nFOG and the NCs did not show significant differences (Fig. 2b).

3.4. Disrupted rich-club functional organization in PD-FOG

As the network was fully connected for all three groups at a sparsity of 29%, rich-club measures were extracted and compared between groups only at this S. All three groups exhibited a presence of the rich-club organization. Statistically significantly ($p_{corr}<0.05$) weaker rich-club edge strength and feeder edge strength were found in PD-FOG when compared to both PD-nFOG and NC participants (Fig. 3a, b). The PD-FOG participants had a significantly higher local edge strength compared to the PD-NFOG and NCs (Fig. 3c). No differences were observed between the PD-NFOG and NCs.

No significant correlations were found between any of the functional network measures and disease duration or MDS-UPRDRS-III “ON” score.

4. Discussion

We utilized high-temporal resolution rs-fMRI data to investigate brain functional network topology in PD patients with and without FOG. FOG in PD is considered as one of the most debilitating motor symptoms that affect almost 50% of PD patients (Amboni et al., 2015; Macht et al., 2007). FOG is one of the most common causes of falls and subsequently contributes to significantly impaired quality of life. A better understanding of PD-FOG may promote the development of therapeutic modalities to treat this disorder since existing treatment options are limited and often not very effective.

The main objective of this study was to assess changes in global network measures and to evaluate changes in brain networks in PD-FOG participants when compared to PD-nFOG and NCs.

4.1. Global functional network changes in PD-FOG

We found that the PD-FOG participants showed significantly altered global functional connectivity compared to the PD-nFOG and NCs. Graph-theoretical studies have shown that functional networks are structured in a well-organized small-world manner reflecting an optimized healthy brain network organization (Achard and Bullmore, 2007). A disturbance of this organization could in turn be associated with brain function differences in healthy and diseased states (Achard and Bullmore, 2007; He et al., 2008). Our results showed that all groups have a small-world organization of brain networks ($\sigma >> 1$).

However, the measures of small-worldness were significantly increased in PD-FOG as compared to the PD-nFOG and NCs. Specifically, in the PD-FOG participants, the clustering coefficient was significantly higher when compared to the PD-nFOG and the NCs, with a similar reduction in the path length. In contrast to the observations in the healthy individuals where sparse small-world networks are responsible for efficient information transfer (Bullmore and Sporns, 2009), in PD-FOG the exaggerated small-world property could be associated with abnormal network function. We speculate that the increased clustering coefficient and reduction in path length becomes a deterrent in PD-FOG wherein a) the networks are more “regular network” rather than a “small-world network” with reduced network strength; b) networks are unable to efficiently transfer the information as might be observed by the reduced global and local efficiency and c) the between network communication is significantly affected as might be seen by the significantly lower assortativity and an increased clustering coefficient. Indeed, the increase in small-worldness due to an increased clustering coefficient in the PD-FOG participants when compared to both, the PD-nFOG and NCs were accompanied by a significant reduction in several other network measures such as global and local efficiency, network strength, and lower assortativity.

These results are in agreement with earlier metabolic studies in both humans and nonhuman primates that have reported increased small-world properties in PD (Ko et al., 2018; Peng et al., 2016). These studies investigated the metabolic demands of certain subnetworks and found that in both humans and nonhuman primates, increased small-worldness within the subgraphs is accompanied by dysfunction (reduced connectivity and efficiency) in other brain networks associated with higher-level functioning. these studies confirm that the usual trend where the loss of network “small-worldness” that are observed in patients with schizophrenia, mild cognitive impairment, and Alzheimer’s disease (Dicks et al., 2018; He

et al., 2009; Kambeitz et al., 2016) is not seen in PD-FOG. We speculate that this exaggerated small-world property and reduction in global network properties could be due to the increasing demand faced by different cognitive networks to compensate for the motor dysfunction. As a result, this disrupts the within-network connectivity and between-network connectivity that subsequently affects the ability to set-shift between different networks and increases the risk of FOG.

Of note, the small-world properties were not significantly different between the PD-nFOG and the NC participants further bolstering our hypothesis of metabolic dysfunction in PD-FOG.

4.2. Insights into the reorganization of the complex brain networks

In line with the observed alternations in the global network measures in the PD-FOG participants, there was also a marked reorganization of 'hub' regions as revealed by the hub disruption index. This nodal reorganization was not significantly different when comparing NCs and PD-nFOG participants. The comparison between NCs and the PD-FOG participants showed that parietal and occipital regions with high nodal connectivity (hub regions) exhibited greatly reduced functional interactions (non-hub-like), while the frontal regions demonstrated a notable increase (hub-like) in their functional interactions in the FOG participants. However, more importantly, compared to the PN-nFOG group, regions that are part of the primary somatosensory, motor (e.g. postcentral gyrus, paracentral lobule) and visuomotor coordination areas (e.g. superior parietal lobule) showed a substantial reduction in hubness in the PD-FOG participants. Furthermore, regions belonging to the prefrontal cortex namely the superior frontal, middle frontal, and inferior frontal regions showed an increase in their hubness in PD-FOG compared to PD-nFOG participants.

Several neuroimaging studies have consistently identified structural and functional changes in several frontal regions and impairment of the frontoparietal network as a key mechanism pertinent to the development of FOG in PD patients (Bharti et al., 2019). Evidence from several clinical and neuropsychological studies also shows that PD-FOG correlates with aberrations in executive functions such as response inhibition, problem-solving, and divided or switching attention (Bharti et al., 2019; Bluett et al., 2018). Divided or switching attention plays a relevant role in locomotion (Mirelman et al., 2018) and subsequently, executive and attention deficits could contribute to deficits in set-shifting and therefore to FOG during tasks involving high cognitive demand. The results of our study also indicate a significant increase in hubness in the regions that are part of the prefrontal cortex and can be attributed to increased demand in cortical functioning due to deficits in movement automaticity in PD-FOG (Nieuwboer and Giladi, 2013). As one of the networks that are heavily involved in cognition, frontoparietal network dysfunction has been consistently associated with FOG in PD. Significant alterations in bold response and functional connectivity among the regions that are part of the frontoparietal network (FPN) have been reported in PD-FOG (Bharti et al., 2019; Shine et al., 2013b).

Given previous evidence that FPN may serve as a flexible hub that alters functional connectivity with other neural networks based on task requirements (Cole et al., 2013), as well as its proposed role in

cognitive and executive functioning which is associated with PD-FOG (Zanto and Gazzaley, 2013), the observed changes in hub-like characteristics of several frontal and parietal regions in the PD-FOG group in our study indicate the importance of these regions in the communication between the different neural networks in situations of increased cognitive demands during gait. Hub regions not only play an important role in localized information processing (segregation) but are involved in the integration of information across the cortical brain network (van den Heuvel and Sporns, 2013). The organizational properties of the hubs can be studied by the 'rich-club' phenomenon where hubs of a network tend to be more connected to similar nodes (hubs) rather than nodes of a lower degree (non-hubs) (van den Heuvel and Sporns, 2011).

The rich-club organization can provide important information related to the higher-order topological organization of the brain functional networks. To this end, we observed that all three groups (PD-FOG, PD-nFOG, and NC) showed the existence of the rich-club organization. However, there was a significant decrease in the rich-club edge strength and feeder edge strength in the PD-FOG group when compared to the PD-nFOG and NC groups. The local connectivity (the connection between non-hubs) was significantly higher in the PD-FOG group when compared to the other groups. In parallel with the reduced network efficiency and reorganization of hubs, the reduced rich-club connectivity indicates a disturbance in between network integration required for higher-level functions. These results highlight the failure in effective integration of information between these hub regions leading to deficits in dual-tasking ability or inability to "set-shift" among the different neural networks. Existing evidence on the alterations of the brains' functional rich-club organization in neurodegenerative disorders (Dicks et al., 2018; He et al., 2009; Kambeitz et al., 2016) further supports the importance of studying the higher-level architectural organization of the brain in PD-FOG.

Limitations of this study should be noted. First, FOG in PD is a complex issue on multiple levels and recognizing that it is not a uniform and homogeneous symptom is crucial to gaining a better understanding of its pathophysiology (Amboni et al., 2015). FOG can be classified based on response to medication as follows a) levodopa-responsive (FOG only in the "OFF" state), b) levodopa-unresponsive and c) levodopa-induced (FOG only in the "ON" state) (Amboni et al., 2015; Espay et al., 2012; Fasano and Lang, 2015). In this study, we did not classify the PD patients based on response to medication, but to be able to further understand the pathophysiology and the different pharmacological FOG subtypes. Hence future studies should compare the different subtypes. Second, our PD-FOG group had a higher MDS-UPDRS-III "ON" score when compared to the PD-nFOG group. However, we believe that our results are not primarily driven by this since a) the two groups were not significantly different in age, PD duration, change in MDS-UPDRS-III between "OFF" and "ON" states (Δ_{OFF-ON}PD-FOG = 12.56 ± 7.32; Δ_{OFF-ON}PD-nFOG = 9.56 ± 4.46;p-value = 0.22) or Hoehn and Yahr stage and b) earlier studies have shown that higher disability (measured by MDS-UPDRS-III scores) are clinical features of FOG (Amboni et al., 2015). However, these findings point to measures and outcomes to be further explored with more closely matched samples to further understand the biology of FOG. Third, there is a possibility that changes in the 'hubness' of frontal and parietal regions seen in PD-FOG participants could be associated with

cognitive decline. While our PD-FOG and PD-nFOG participants showed no differences in the MoCA scores our study did not conduct a detailed evaluation of the relationship between network changes and cognition. Finally, we did not observe any statistically significant relationship between the network measures and clinical measures. However, a weak correlation and difference in the relationship ($p_{uncorr} < 0.05$; moderate effect $r > 0.3$) were observed between path length and hub index with the MDS-UPDRS III "ON" scores (Suppl. Figure 2). Therefore, further follow-up studies of larger sample sizes with deeper phenotyping are required to confirm our findings. Such studies may allow the detection of significant differences and relationships between connectivity and behavior (including detailed cognitive assessments) that were not observed in the current data set.

Future directions to be explored to gain further understanding of the pathophysiology of FOG include: a) elucidation of FOG subtypes based on rs-FC and network topology, b) studying the effect of levodopa by comparing 'ON' and 'OFF' state network topology in PD-FOG, c) examination of the FC during the performance of specific executive-attention tasks, d) incorporating advanced analytical methods like dynamic FC (Zhuang et al., 2018) and empirical mode decomposition (Cordes et al., 2021, 2018); and (e) joint analysis of structural network connectivity disturbance (Mishra et al., 2019) and functional network connectivity disturbance.

In summary, the results of our study demonstrate that PD-FOG participants exhibit different pathophysiology compared to PD-nFOG and NC due to the significant alteration in the global network properties and substantial reorganization of regional brain hubs. In addition, there was a significant reduction in the rich-club connectivity strength in the PD-FOG participants suggestive of disruptions in the higher-order functional network topology.

Declarations

No competing financial interests exist relevant to this study.

Author Contributions

(1) A. Conception and design of the study, B. Acquisition of data, C. Analysis and interpretation of data, (2) A. Drafting the article, B. Revising it critically for important intellectual content, (3) Final approval of the version to be submitted.

K.S.: 1B, 1C, 2A, 2B, 3.

E.B.: 1B, 1C, 2B, 3

X.Z.: 1C, 2B, 3

J.L.: 1B, 1C, 2B, 3

Z.Y.: 1C, 2B, 3

D.C.: 1C, 2B, 3

A.R.: 1B, 2B, 3

J.C.: 1B, 2B, 3

J.L.C.: 1C, 2B, 3

Z.M..: 1C, 2B, 3

I.L.: 1A, 1C, 2B, 3

B.B.: 1A, 1C, 2B, 3

V.M.: 1A, 1B, 1C, 2B, 3

Acknowledgments

This study was supported by the NIH (grant R01NS117547, grant 1RF1AG071566, and COBRE grant 1P20GM109025-01A1), a private grant from the Elaine P Wynn and Family Foundation, a private grant from the Peter and Angela Dal Pezzo funds, a private grant from Lynn and William Weidner, a private grant from Stacie and Chuck Matthewson and the Keep Memory Alive-Young Investigator Award.

References

1. Achard, S., Bullmore, E., 2007. Efficiency and cost of economical brain functional networks. PLoS Comput. Biol. 3, 0174–0183. https://doi.org/10.1371/journal.pcbi.0030017
2. Achard, S., Delon-Martin, C., Vértes, P.E., Renard, F., Schenck, M., Schneider, F., Heinrich, C., Kremer, S., Bullmore, E.T., 2012. Hubs of brain functional networks are radically reorganized in comatose patients. Proc. Natl. Acad. Sci. U. S. A. 109, 20608–20613. https://doi.org/10.1073/pnas.1208933109
3. Achard, S., Salvador, R., Whitcher, B., Suckling, J., Bullmore, E., 2006. A resilient, low-frequency, small-world human brain functional network with highly connected association cortical hubs. J. Neurosci. 26, 63–72. https://doi.org/10.1523/JNEUROSCI.3874-05.2006
4. Allen, N.E., Schwarzel, A.K., Canning, C.G., 2013. Recurrent falls in parkinson's disease: A systematic review. Parkinsons. Dis. 2013. https://doi.org/10.1155/2013/906274
5. Amboni, M., Stocchi, F., Abbruzzese, G., Morgante, L., Onofrj, M., Ruggieri, S., Tinazzi, M., Zappia, M., Attar, M., Colombo, D., Simoni, L., Ori, A., Barone, P., Antonini, A., 2015. Prevalence and associated features of self-reported freezing of gait in Parkinson disease: The DEEP FOG study. Park. Relat. Disord. 21, 644–649. https://doi.org/10.1016/j.parkreldis.2015.03.028

6. Bachmann, C., Jacobs, H.I.L., Porta Mana, P., Dillen, K., Richter, N., von Reutern, B., Dronse, J., Onur, O.A., Langen, K.-J., Fink, G.R., Kukolja, J., Morrison, A., 2018. On the Extraction and Analysis of Graphs From Resting-State fMRI to Support a Correct and Robust Diagnostic Tool for Alzheimer's Disease. Front. Neurosci. 12, 528. https://doi.org/10.3389/fnins.2018.00528
7. Bassett, D.S., Bullmore, E., Verchinski, B.A., Mattay, V.S., Weinberger, D.R., Meyer-Lindenberg, A., 2008. Hierarchical organization of human cortical networks in health and Schizophrenia. J. Neurosci. 28, 9239–9248. https://doi.org/10.1523/JNEUROSCI.1929-08.2008
8. Behzadi, Y., Restom, K., Liau, J., Liu, T.T., 2007. A component based noise correction method (CompCor) for BOLD and perfusion based fMRI. Neuroimage 37, 90–101. https://doi.org/10.1016/j.neuroimage.2007.04.042
9. Bharti, K., Suppa, A., Tommasin, S., Zampogna, A., Pietracupa, S., Berardelli, A., Pantano, P., 2019. Neuroimaging advances in Parkinson's disease with freezing of gait: A systematic review. NeuroImage Clin. 24, 102059. https://doi.org/10.1016/j.nicl.2019.102059
10. Bluett, B., Banks, S., Cordes, D., Bayram, E., Mishra, V., Cummings, J., Litvan, I., 2018. Neuroimaging and neuropsychological assessment of freezing of gait in Parkinson's disease. Alzheimer's Dement. Transl. Res. Clin. Interv. 4, 387–394. https://doi.org/10.1016/j.trci.2018.04.010
11. Browner, N., Giladi, N., 2010. What can we learn from freezing of gait in Parkinson's disease? Curr. Neurol. Neurosci. Rep. 10, 345–351. https://doi.org/10.1007/S11910-010-0127-1/TABLES/1
12. Bullmore, E., Sporns, O., 2009. Complex brain networks: Graph theoretical analysis of structural and functional systems. Nat. Rev. Neurosci. 10, 186–198. https://doi.org/10.1038/nrn2575
13. Caeyenberghs, K., Verhelst, H., Clemente, A., Wilson, P.H., 2017. Mapping the functional connectome in traumatic brain injury: What can graph metrics tell us? Neuroimage 160, 113–123. https://doi.org/10.1016/j.neuroimage.2016.12.003
14. Caliandro, P., Vecchio, F., Miraglia, F., Reale, G., Della Marca, G., La Torre, G., Lacidogna, G., Iacovelli, C., Padua, L., Bramanti, P., Rossini, P.M., 2017. Small-World Characteristics of Cortical Connectivity Changes in Acute Stroke. Neurorehabil. Neural Repair 31, 81–94. https://doi.org/10.1177/1545968316662525
15. Cao, M., Huang, H., He, Y., 2017. Developmental Connectomics from Infancy through Early Childhood. Trends Neurosci. 40, 494–506. https://doi.org/10.1016/j.tins.2017.06.003
16. Cole, M.W., Reynolds, J.R., Power, J.D., Repovs, G., Anticevic, A., Braver, T.S., 2013. Multi-task connectivity reveals flexible hubs for adaptive task control. Nat. Neurosci. 16, 1348–1355. https://doi.org/10.1038/nn.3470
17. Cordes, D., Kaleem, M.F., Yang, Z., Zhuang, X., Curran, T., Sreenivasan, K.R., Mishra, V.R., Nandy, R., Walsh, R.R., 2021. Energy-Period Profiles of Brain Networks in Group fMRI Resting-State Data: A Comparison of Empirical Mode Decomposition With the Short-Time Fourier Transform and the Discrete Wavelet Transform. Front. Neurosci. 15, 594. https://doi.org/10.3389/FNINS.2021.663403/BIBTEX

18. Cordes, D., Zhuang, X., Kaleem, M., Sreenivasan, K., Yang, Z., Mishra, V., Banks, S.J., Bluett, B., Cummings, J.L., 2018. Advances in functional magnetic resonance imaging data analysis methods using Empirical Mode Decomposition to investigate temporal changes in early Parkinson's disease. Alzheimer's Dement. Transl. Res. Clin. Interv. 4, 372–386. https://doi.org/10.1016/j.trci.2018.04.009
19. Dicks, E., Tijms, B.M., ten Kate, M., Gouw, A.A., Benedictus, M.R., Teunissen, C.E., Barkhof, F., Scheltens, P., van der Flier, W.M., 2018. Gray matter network measures are associated with cognitive decline in mild cognitive impairment. Neurobiol. Aging 61, 198–206. https://doi.org/10.1016/j.neurobiolaging.2017.09.029
20. Espay, A.J., Fasano, A., Van Nuenen, B.F.L., Payne, M.M., Snijders, A.H., Bloem, B.R., 2012. "On" state freezing of gait in Parkinson disease: A paradoxical levodopa-induced complication. Neurology 78, 454–457. https://doi.org/10.1212/WNL.0b013e3182477ec0
21. Fan, L., Li, H., Zhuo, J., Zhang, Y., Wang, J., Chen, L., Yang, Z., Chu, C., Xie, S., Laird, A.R., Fox, P.T., Eickhoff, S.B., Yu, C., Jiang, T., 2016. The Human Brainnetome Atlas: A New Brain Atlas Based on Connectional Architecture. Cereb. Cortex 26, 3508–3526. https://doi.org/10.1093/cercor/bhw157
22. Fasano, A., Herman, T., Tessitore, A., Strafella, A.P., Bohnen, N.I., 2015. Neuroimaging of freezing of gait. J. Parkinsons. Dis. 5, 241–254. https://doi.org/10.3233/JPD-150536
23. Fasano, A., Lang, A.E., 2015. Unfreezing of gait in patients with Parkinson's disease. Lancet Neurol. 14, 675–677. https://doi.org/10.1016/S1474-4422(15)00053-8
24. Gleichgerrcht, E., Kocher, M., Bonilha, L., 2015. Connectomics and graph theory analyses: Novel insights into network abnormalities in epilepsy. Epilepsia 56, 1660–1668. https://doi.org/10.1111/epi.13133
25. Guo, M.R., Ren, Y., Yu, H.M., Yang, H.G., Cao, C.H., Li, Y.M., Fan, G.G., 2020. Alterations in Degree Centrality and Functional Connectivity in Parkinson's Disease Patients With Freezing of Gait: A Resting-State Functional Magnetic Resonance Imaging Study. Front. Neurosci. 14. https://doi.org/10.3389/fnins.2020.582079
26. He, Y., Chen, Z., Evans, A., 2008. Structural insights into aberrant topological patterns of large-scale cortical networks in Alzheimer's disease. J. Neurosci. 28, 4756–4766. https://doi.org/10.1523/JNEUROSCI.0141-08.2008
27. He, Y., Chen, Z., Gong, G., Evans, A., 2009. Neuronal networks in Alzheimer's disease. Neuroscientist 15, 333–350. https://doi.org/10.1177/1073858409334423
28. Kambeitz, J., Kambeitz-Ilankovic, L., Cabral, C., Dwyer, D.B., Calhoun, V.D., Van Den Heuvel, M.P., Falkai, P., Koutsouleris, N., Malchow, B., 2016. Aberrant Functional Whole-Brain Network Architecture in Patients with Schizophrenia: A Meta-analysis. Schizophr. Bull. 42, S13–S21. https://doi.org/10.1093/schbul/sbv174
29. Ko, J.H., Spetsieris, P.G., Eidelberg, D., 2018. Network structure and function in Parkinson's disease. Cereb. Cortex 28, 4121–4135. https://doi.org/10.1093/cercor/bhx267
30. Li, N., Suo, X., Zhang, J., Lei, D., Wang, L., Li, J., Peng, J., Duan, L., Gong, Q., Peng, R., 2021. Disrupted functional brain network topology in Parkinson's disease patients with freezing of gait. Neurosci.

Lett. 759. https://doi.org/10.1016/j.neulet.2021.135970

31. Macht, M., Kaussner, Y., Möller, J.C., Stiasny-Kolster, K., Eggert, K.M., Krüger, H.P., Ellgring, H., 2007. Predictors of freezing in Parkinson's disease: A survey of 6,620 patients. Mov. Disord. 22, 953–956. https://doi.org/10.1002/MDS.21458
32. Maidan, I., Jacob, Y., Giladi, N., Hausdorff, J.M., Mirelman, A., 2019. Altered organization of the dorsal attention network is associated with freezing of gait in Parkinson's disease. Park. Relat. Disord. 63, 77–82. https://doi.org/10.1016/j.parkreldis.2019.02.036
33. Mirelman, A., Shema, S., Maidan, I., Hausdorff, J.M., 2018. Gait. Handb. Clin. Neurol. 159, 119–134. https://doi.org/10.1016/B978-0-444-63916-5.00007-0
34. Mishra, V.R., Sreenivasan, K.R., Yang, Z., Zhuang, X., Cordes, D., Mari, Z., Litvan, I., Fernandez, H.H., Eidelberg, D., Ritter, A., Cummings, J.L., Walsh, R.R., 2020. Unique white matter structural connectivity in early-stage drug-naive Parkinson disease. Neurology 94. https://doi.org/10.1212/WNL.0000000000008867
35. Naismith, S.L., Shine, J.M., Lewis, S.J.G., 2010. The specific contributions of set-shifting to freezing of gait in Parkinson's disease. Mov. Disord. 25, 1000–1004. https://doi.org/10.1002/mds.23005
36. Newman, M.E.J., 2002. Assortative Mixing in Networks. Phys. Rev. Lett. 89. https://doi.org/10.1103/PhysRevLett.89.208701
37. Nieuwboer, A., Giladi, N., 2013. Characterizing freezing of gait in Parkinson's disease: Models of an episodic phenomenon. Mov. Disord. 28, 1509–1519. https://doi.org/10.1002/mds.25683
38. Peng, S., Ma, Y., Flores, J., Cornfeldt, M., Mitrovic, B., Eidelberg, D., Doudet, D.J., 2016. Modulation of abnormal metabolic brain networks by experimental therapies in a nonhuman primate model of Parkinson disease: An application to human retinal pigment epithelial cell implantation. J. Nucl. Med. 57, 1591–1598. https://doi.org/10.2967/jnumed.115.161513
39. Perry, A., Wen, W., Lord, A., Thalamuthu, A., Roberts, G., Mitchell, P.B., Sachdev, P.S., Breakspear, M., 2015. The organisation of the elderly connectome. Neuroimage 114, 414–426. https://doi.org/10.1016/j.neuroimage.2015.04.009
40. Rocca, M.A., Valsasina, P., Meani, A., Falini, A., Comi, G., Filippi, M., 2016. Impaired functional integration in multiple sclerosis: a graph theory study. Brain Struct. Funct. 221, 115–131. https://doi.org/10.1007/s00429-014-0896-4
41. Ruan, X., Li, Y., Li, E., Xie, F., Zhang, G., Luo, Z., Du, Y., Jiang, X., Li, M., Wei, X., 2020. Impaired Topographical Organization of Functional Brain Networks in Parkinson's Disease Patients With Freezing of Gait. Front. Aging Neurosci. 12, 337. https://doi.org/10.3389/fnagi.2020.580564
42. Rubinov, M., Sporns, O., 2010. Complex network measures of brain connectivity: Uses and interpretations. Neuroimage 52, 1059–1069. https://doi.org/10.1016/j.neuroimage.2009.10.003
43. Shine, J.M., Matar, E., Ward, P.B., Frank, M.J., Moustafa, A.A., Pearson, M., Naismith, S.L., Lewis, S.J.G., 2013a. Freezing of gait in Parkinson's disease is associated with functional decoupling between the cognitive control network and the basal ganglia. Brain 136, 3671–3681. https://doi.org/10.1093/BRAIN/AWT272

44. Shine, J.M., Moustafa, A.A., Matar, E., Frank, M.J., Lewis, S.J.G., 2013b. The role of frontostriatal impairment in freezing of gait in Parkinson's disease. Front. Syst. Neurosci. 7. https://doi.org/10.3389/fnsys.2013.00061
45. Snijders, A.H., Leunissen, I., Bakker, M., Overeem, S., Helmich, R.C., Bloem, B.R., Toni, I., 2011. Gait-related cerebral alterations in patients with Parkinson's disease with freezing of gait. Brain 134, 59–72. https://doi.org/10.1093/BRAIN/AWQ324
46. Sporns, O., Tononi, G., Kötter, R., 2005. The human connectome: A structural description of the human brain. PLoS Comput. Biol. 1, 0245–0251. https://doi.org/10.1371/journal.pcbi.0010042
47. Sreenivasan, K., Mishra, V., Bird, C., Zhuang, X., Yang, Z., Cordes, D., Walsh, R.R.R., 2019. Altered functional network topology correlates with clinical measures in very early-stage, drug-naïve Parkinson's disease. Park. Relat. Disord. 62, 3–9. https://doi.org/10.1016/j.parkreldis.2019.02.001
48. van den Heuvel, M.P., Sporns, O., 2013. Network hubs in the human brain. Trends Cogn. Sci. 17, 683–696. https://doi.org/10.1016/j.tics.2013.09.012
49. van den Heuvel, M.P., Sporns, O., 2011. Rich-club organization of the human connectome. J. Neurosci. 31, 15775–15786. https://doi.org/10.1523/JNEUROSCI.3539-11.2011
50. Wang, J., Wang, X., Xia, M., Liao, X., Evans, A., He, Y., 2015. GRETNA: A graph theoretical network analysis toolbox for imaging connectomics. Front. Hum. Neurosci. 9, 386. https://doi.org/10.3389/fnhum.2015.00386
51. Watts, D.J., Strogatz, S.H., 1998. Collective dynamics of 'small-world9 networks. Nature 393, 440–442. https://doi.org/10.1038/30918
52. Winkler, A.M., Ridgway, G.R., Webster, M.A., Smith, S.M., Nichols, T.E., 2014. Permutation inference for the general linear model. Neuroimage 92, 381–397. https://doi.org/10.1016/j.neuroimage.2014.01.060
53. Zanto, T.P., Gazzaley, A., 2013. Fronto-parietal network: Flexible hub of cognitive control. Trends Cogn. Sci. 17, 602–603. https://doi.org/10.1016/j.tics.2013.10.001
54. Zhuang, X., Walsh, R.R., Sreenivasan, K., Yang, Z., Mishra, V., Cordes, D., 2018. Incorporating spatial constraint in co-activation pattern analysis to explore the dynamics of resting-state networks: An application to Parkinson's disease. Neuroimage 172, 64–84. https://doi.org/10.1016/j.neuroimage.2018.01.019
55. Ziegler, K., Schroeteler, F., Ceballos-Baumann, A.O., Fietzek, U.M., 2010. A new rating instrument to assess festination and freezing gait in Parkinsonian patients. Mov. Disord. 25, 1012–1018. https://doi.org/10.1002/mds.22993

Figures

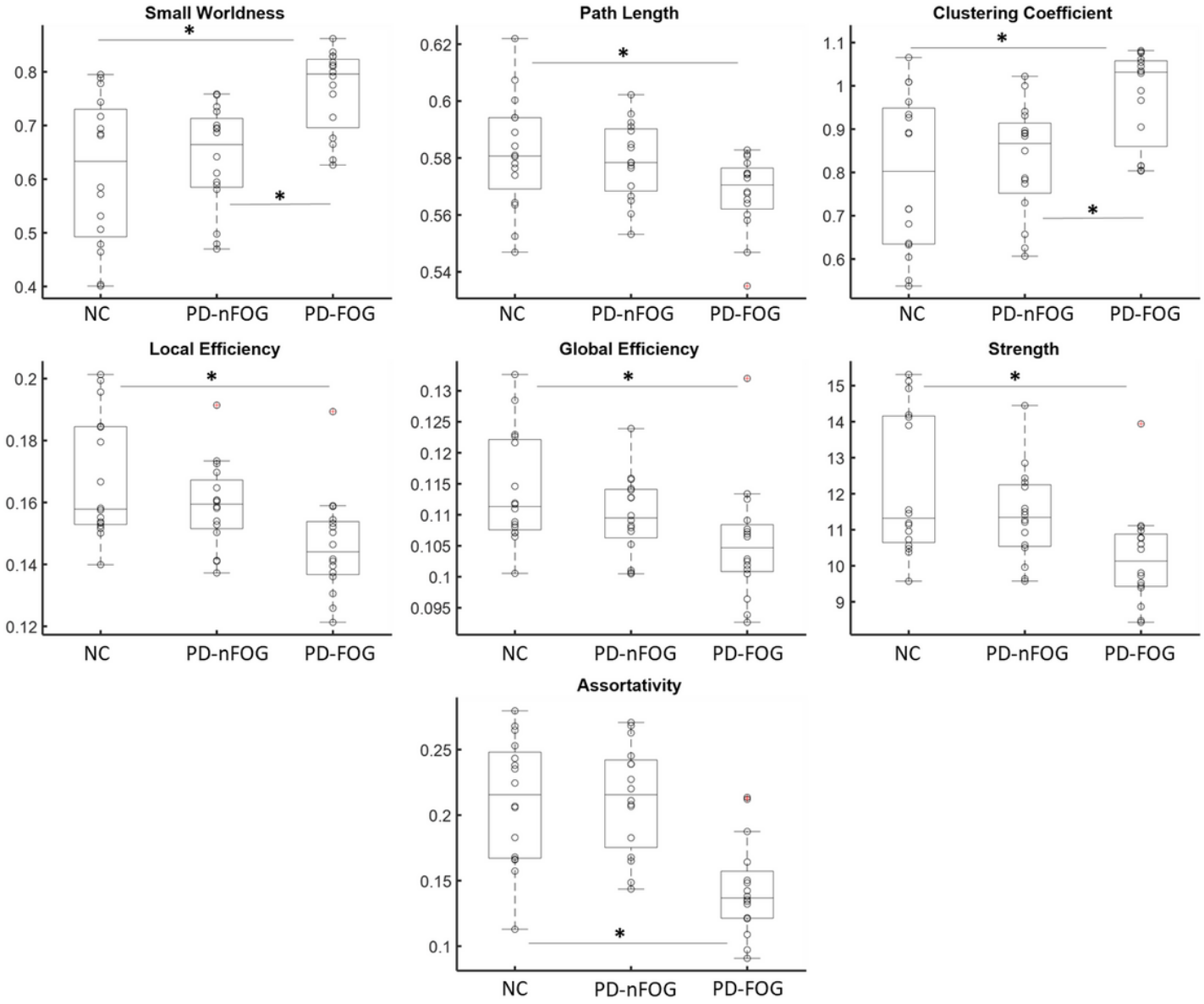

Figure 1

Global network metrics in the study groups. (a) Small-worldness (b) Path length (c) Clustering coefficient (d) Global efficiency (e) Local efficiency (e) Strength and (g) Assortativity. * indicates significant (p_{corr}<0.05) difference. The right panel indicates the relationship between overall network path length, global and local efficiency, and MDS-UPDRS III scores.

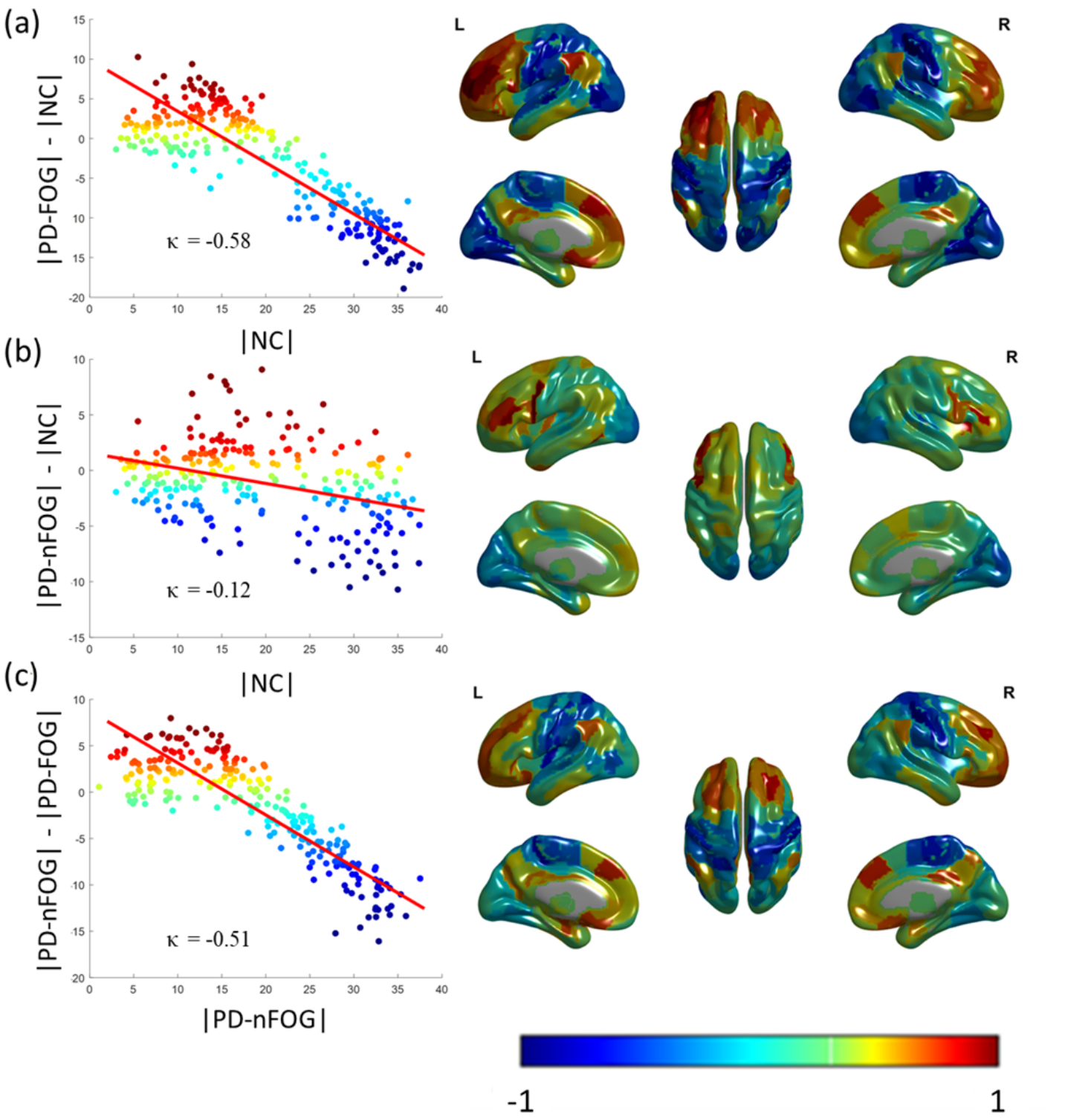

Figure 2

The hub regions were significantly reorganized in the PD-FOG participants. The mean degree of each node in the reference group (x-axis) is plotted versus the difference between the mean degree of each node of the reference group and chosen group (y-axis). κ was calculated as the slope of the line (shown in red) fitted to the scatterplot (a) Reference group: Control (NC); Chosen group: PD-FOG (b) Reference group: NC; Chosen group: PD-nFOG and (c) Reference group: PD-nFOG; Chosen group: PD-FOG. The red

color denotes increased hubness, on average, in the chosen group compared to the reference group; blue denotes abnormally decreased hubness in the chosen group. The right panel in each of the sub-figures is the cortical surface representation of the difference in mean degree between the reference and chosen group and are the colors are the same as in the scatter plot. L: Left and R: Right.

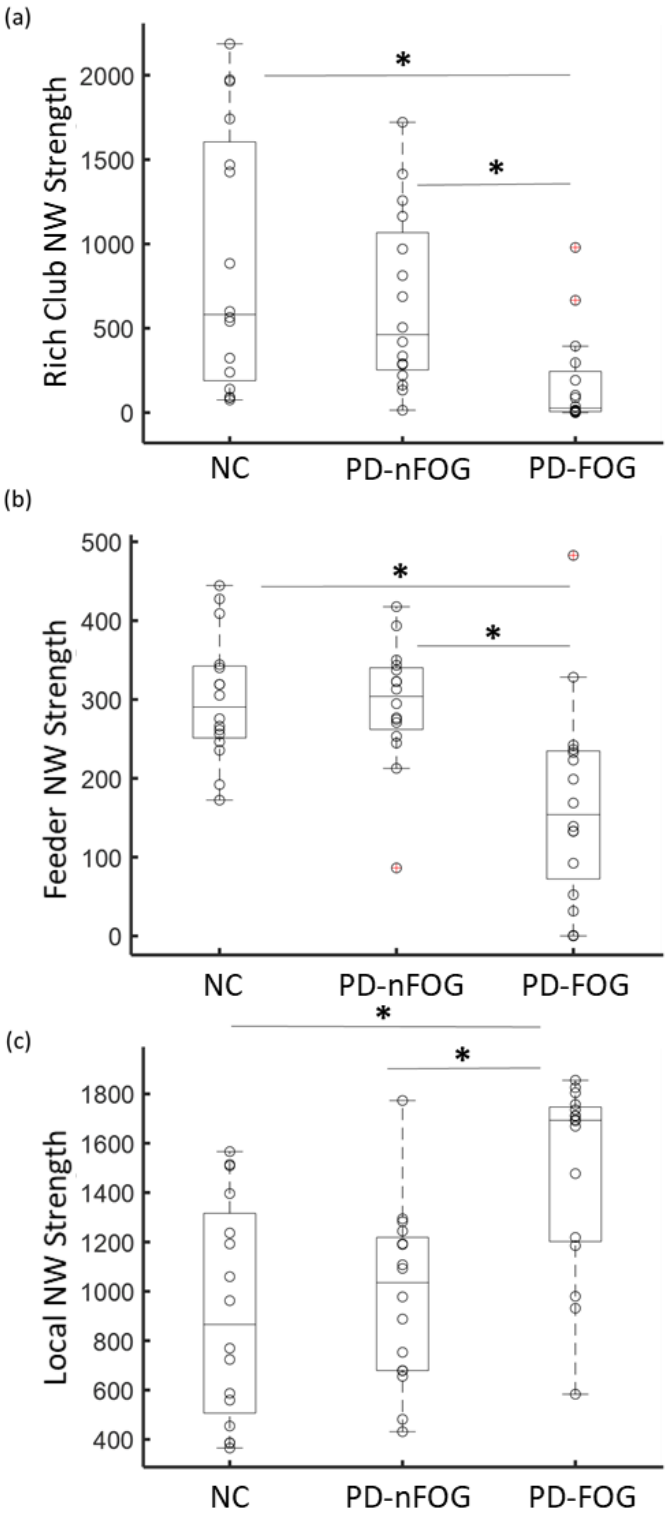

Figure 3

Rich-club connectivity in the three study groups. Rich-club network strength, feeder network strength, and local network strength are plotted as bar plots for NC, PD-nFOG, and PD-FOG participants. Rich-club network – edges between rich-club nodes; feeder network – edges connecting non-rich-club nodes and rich club nodes; local network – edges between non-rich-club nodes. * indicates statistical significance ($p < 0.05$).

Supplementary Files

This is a list of supplementary files associated with this preprint. Click to download.

- SupplementaryFigures.docx